

Serial and parallel arrangements of NOLM and NALM loop mirrors

Diethelm Schmieder and Pieter L. Swart

University of Johannesburg, Johannesburg, South Africa

We present the switching equations for the nonlinear optical loop mirror (NOLM), for two NOLM loops in series, for two NOLM loops in parallel, for the nonlinear amplifying loop mirror (NALM), for two NALM loops in series, and for two NALM loops in parallel. We investigate the switching behavior of arrangements of two identical and two different NOLM loops in dependence of the length of the nonlinear Kerr fiber, the effective fiber core area and the coupling constant. The same investigations are carried out with two identical and two different NALM loops, where additionally the dependence of the gain is considered. The coupling constant α is kept fixed at 0.5.

OCIS codes: 060.0060, 060.4370.

Rare-earth doped optical fibers offer wide gain bandwidths and provide an ideal medium for the generation of ultrashort optical pulses. For example the Er^{3+} -doped optical fiber laser has a bandwidth of approximately 30 nm. Passive mode-locking has been demonstrated in figure-eight lasers in the nonlinear optical loop mirror (NOLM)^[1] and nonlinear amplifying loop mirror (NALM) configuration. Depending on the pumping power different modes of pulse generation have been observed. At low pumping powers the loop mirrors are operating in Q -switching mode. As the pump power increases, above a certain threshold, the laser operates in mode-locking mode, and single pulses are observed per cavity round-trip. At even higher pump powers multiple pulses appear per cavity round-trip and the laser becomes unstable^[2]. To overcome these problems, we investigate the switching behavior in different NOLM-NOLM or NALM-NALM loop mirror configurations.

The NOLM was first proposed by Doran *et al.*^[1]. It is a fast optical switch. Its switching property is based on the nonlinear phase induced by self-phase modulation (SPM). The splitting ratio of the coupler is $\alpha \neq 0.5$, therefore the counter-propagating beams experience different phase shifts. In a NALM a short optical amplifier, typically a rare-earth-doped fiber like Er^{3+} , Yb^{3+} , $\text{Er}^{3+}/\text{Yb}^{3+}$, Nd^{3+} , Ho^{3+} , Tl^{3+} , Pr^{3+} is spliced into a long fiber loop. The amplifier is positioned at one end of the loop, close to the coupler. The coupler has a splitting ratio of $\alpha = 0.5$. Since the fiber amplifier is placed at one end of the loop, at high optical input powers the nonlinear refractive Kerr index leads to a change in the optical path lengths for light propagating clockwise and counterclockwise around the loop and to different phases of the two counter-propagating fields. If no polarization controllers are inserted, polarization rotation inside the loop is responsible for a further intensity dependent phase difference between the two paths^[2].

The NALM loop mirror is shown in Fig. 1. The NOLM loop mirror is identical, except the Er^{3+} -doped fiber is absent, and the coupling ratio is not 50%. The linear and nonlinear refractive index in the fiber loop is $n = n_0 + \frac{n_2 |E|^2 L}{A_{\text{eff}}}$, where n_0 is the linear refractive index, $|E|^2$ is the intensity, L is the length of the nonlinear Kerr fiber in the loop, and A_{eff} is the effective fiber core area. The phase of the two fields is $\Phi = kL = \frac{2\pi}{\lambda} nL$, where k is the wave number and λ the wavelength. The

linear refractive index is the same for all the fields and cancels out. The phase shift acquired by a field E propagating a distance L under the influence of self-phase modulation (SPM) is $\Phi = \frac{2\pi n_2 |E|^2 L}{A_{\text{eff}} \lambda} = \frac{N_L |E|^2 L}{A_{\text{eff}}}$, where $n_2 = 3.2 \times 10^{-23} \frac{\text{m}^2}{\text{mW}}$, $\lambda = 1.55 \mu\text{m}$, $N_L = \frac{2\pi n_2 L}{\lambda}$.

As soon as the intensities in the gain medium become high, much higher than the saturation intensity $|E_S|^2$, the gain exponent becomes intensity dependent, decreases and approaches zero. $g(|E_{\text{in}}|^2) = \frac{g_0 |E_S|^2}{|E_S|^2 + |E_{\text{in}}|^2}$, where $|E_{\text{in}}|^2$ is the incoming light power, and $|E_S|^2$ the saturation intensity, and it is the intensity at which the gain exponent $g = g_0/2$ ^[3]. We have determined the small signal gain exponent $g_0 = 0.705$, and the saturation intensity $|E_S|^2 = 0.606 \text{ mW}$. We use the simplest gain model which mimics the Beer-Lambert law for absorption. The gain is then $G = \exp(gL_{\text{Er}})$, L_{Er} is the length of the Er^{3+} -doped fiber. Switching equation for a single loop is

$$|E_{\text{out}}|^2 = |E_{\text{in}}|^2 G [1 - 2\alpha(1 - \alpha) \cdot \left(1 + \cos \left([\alpha - G(1 - \alpha)] |E_{\text{in}}|^2 N_L \frac{L}{A_{\text{eff}}} \right) \right)] \quad (1)$$

for the NOLM loop $G = 1$. In all our calculations we ignore losses and the phase shifts in the connecting fibers.

Two NALM loop mirrors in series are shown in Fig. 2. The NOLM loop mirrors are identical, except the Er^{3+} -doped fibers are absent, and the coupling ratio is not 50%. Switching equation for two NALM loops in series is

$$|E_{\text{out1}}|^2 = |E_{\text{in}}|^2 G_1 [1 - 2\alpha_1(1 - \alpha_1) \cdot \left(1 + \cos \left((\alpha_1 - G_1(1 - \alpha_1)) |E_{\text{in}}|^2 N_L \frac{L_1}{A_{\text{eff1}}} \right) \right)] \quad (2)$$

$$|E_{\text{out2}}|^2 = |E_{\text{out1}}|^2 G_2 \cdot \left(1 + \cos \left((\alpha_2 - G_2(1 - \alpha_2)) |E_{\text{out1}}|^2 N_L \frac{L_2}{A_{\text{eff2}}} \right) \right) \quad (3)$$

for the two NOLM loops $G = 1$.

Two NALM loop mirrors in parallel are shown in Fig. 3. The NOLM loop mirrors are identical, except the Er^{3+} -doped fibers are missing, and the coupling ratio is not 50%. Switching equation for two NALM loops in parallel is

$$|E_{\text{out}}|^2 = |E_{\text{in}}|^2 \left(\begin{array}{l} G_1 \alpha_1 \alpha_4 \left(1 - 2\alpha_2(1 - \alpha_2) \left(1 + \cos \left(\alpha_1 (\alpha_2 - G_1(1 - \alpha_2)) |E_{\text{in}}|^2 N_L \frac{L_1}{A_{\text{eff1}}} \right) \right) \right) + G_2(1 - \alpha_1) \\ (1 - \alpha_4) \left(1 - 2\alpha_3(1 - \alpha_3) \left(1 + \cos \left((1 - \alpha_1) (\alpha_3 - G_2(1 - \alpha_3)) |E_{\text{in}}|^2 N_L \frac{L_2}{A_{\text{eff2}}} \right) \right) \right) - \\ - 2\sqrt{G_1 G_2 \alpha_1 (1 - \alpha_1) \alpha_4 (1 - \alpha_4)} \\ \left(\alpha_2 \alpha_3 \cos \left(\left(\alpha_1 \alpha_2 \frac{L_1}{A_{\text{eff1}}} - (1 - \alpha_1) \alpha_3 \frac{L_2}{A_{\text{eff2}}} \right) |E_{\text{in}}|^2 N_L \right) - \right. \\ \left. - \alpha_2(1 - \alpha_3) \cos \left(\left(\alpha_1 \alpha_2 \frac{L_1}{A_{\text{eff1}}} - G_2(1 - \alpha_1)(1 - \alpha_3) \frac{L_2}{A_{\text{eff2}}} \right) |E_{\text{in}}|^2 N_L \right) - \right. \\ \left. - (1 - \alpha_2) \alpha_3 \cos \left(\left(G_1 \alpha_1 (1 - \alpha_2) \frac{L_1}{A_{\text{eff1}}} - (1 - \alpha_1) \alpha_3 \frac{L_2}{A_{\text{eff2}}} \right) |E_{\text{in}}|^2 N_L \right) + \right. \\ \left. + (1 - \alpha_2)(1 - \alpha_3) \right. \\ \left. \cos \left(\left(G_1 \alpha_1 (1 - \alpha_2) \frac{L_1}{A_{\text{eff1}}} - G_2(1 - \alpha_1)(1 - \alpha_3) \frac{L_2}{A_{\text{eff2}}} \right) |E_{\text{in}}|^2 N_L \right) \right) \end{array} \right) \quad (4)$$

for the two NOLM loops $G = 1$. In all our calculations we ignore losses and the phase shifts in the connecting fibers. Reducing the wavelength has the same effect as increasing the length of the Kerr fiber or reducing the effective fiber core area: the Kerr effect is bigger. However, in our investigations we keep the wavelength λ at 1.55 μm . L (L_1, L_2): Length of the highly nonlinear Kerr fiber in a single (the first, second) NOLM or NALM loop; a (a_1, a_2): Radius of the effective fiber core in a single (the first, second) NOLM or NALM loop; α (α_1, α_2): Coupling constant in a single (the first, second) NOLM or NALM loop.

I Simulation results of a single NOLM loop

Figures 4(a)—(c) show the output power versus input power, the ratio of output power/input power versus input power, and the cosine function which is responsible for the switching, respectively. Since we have no gain, the output power is equal to the input power as seen in Fig. 4(a). From Fig. 4(b) we see the modulation depth is almost 100%, because the coupling constant $\alpha = 0.45$. Fig. 4(c) indicates that the output power has a maximum at $\cos = -1$, and a minimum at $\cos = +1$. If we increase the length of the Kerr fiber, reduce the effective fiber core or both, the switching frequency increases.

If we change the coupling constant to $\alpha = 0.15$, the switching frequency increases drastically, but the modulation depth drops to 50% (see Fig. 5).

II Simulation results of two NOLM loops in series

After the first NOLM loop the outputs are identical to those for a single loop. After the second NOLM loop the switching frequency of the first NOLM loop is modulated onto the switching frequency of the second NOLM loop. If we increase the length of the Kerr fiber or reduce the effective area of the first loop, the switching frequency of the first loop increases. If we increase the length of the Kerr fiber or reduce the effective area of the second loop, the modulation switching frequency of the second loop increases (see Fig. 6).

We keep the same fiber parameters, but change the coupling constants of the first and second NOLM loop.

If the coupling constants for both loops are the same, $\alpha = 0.15$, the switching frequency of the first NOLM loop is modulated by the switching frequency of the second loop, as shown in Fig. 7. The modulation depth is 50%. The switching frequency is very much increased compared to $\alpha = 0.45$.

If the coupling constant of the first NOLM loop is 0.45, and the coupling constant of the second loop is 0.15, we get a different modulation pattern, as shown in Fig. 8. The low switching frequency of the first NOLM loop is

modulated by the high switching frequency of the second loop. The modulation depth is 50%.

If we reverse the coupling constants, 0.15 for the first NOLM loop, and 0.45 for the second loop, we get again a different modulation pattern, as shown in Fig. 9. The high switching frequency of the first NOLM loop is modulated by the low switching frequency of the second loop. The modulation depth is 100%.

III Simulation results of two NOLM loops in parallel

If we arrange two equal NOLM loops in parallel, then the switching frequency is halved compared to single loop, and the output power is reduced by a factor of about 2.5.

If we increase in both NOLM loops the lengths of the Kerr fibers or/and decrease the effective fiber core areas, the switching frequency increases, but the output power stays the same (see Fig. 10).

If we increase the length of the nonlinear Kerr fiber and/or reduce the effective core area only of the second loop, we find a modulated switching pattern as shown in Fig. 11. The low switching frequency of the first NOLM loop is modulated by the high switching frequency of the second loop, with the output power slightly lower than the input power. The modulation depth is between 100% and 75%.

If we reverse the settings of the two loops and increase the length of the nonlinear Kerr fiber and/or reduce the effective core area of the first loop, we find a different modulated switching pattern, as shown in Fig. 12. The high switching frequency of the first NOLM loop is modulated by the low switching frequency of the second loop, with the output power slightly lower than the input power. The modulation depth varies between 100% and 65%.

We investigate the coupling ratios of the two parallel NOLM loops. Compared to a single loop, the switching frequency is halved and the output power is reduced by a factor of 2.5. The modulation depth is the same as for a single loop 50%, as shown in Fig. 13.

If we choose for the first NOLM loop the coupling ratio $\alpha = 0.45$ and for the second loop $\alpha = 0.15$, we get a different modulation pattern, as shown in Fig. 14. The low switching frequency of the first NOLM loop is modulated by the higher switching frequency of the second loop. The output power is only slightly lower than the input power, and the modulation depth varies between 100% and 80%.

If we reverse the coupling ratios and choose for the first NOLM loop the coupling ratio $\alpha = 0.15$ and for the

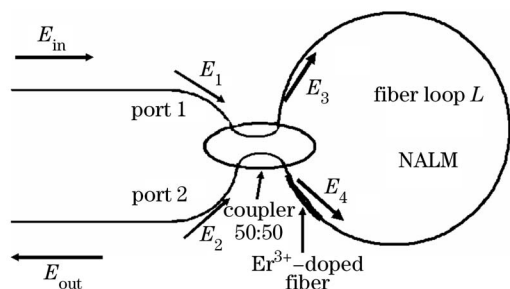


Fig. 1. The NALM configuration.

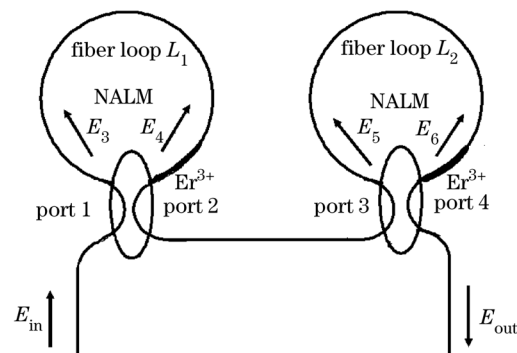


Fig. 2. Two NALMs in series.

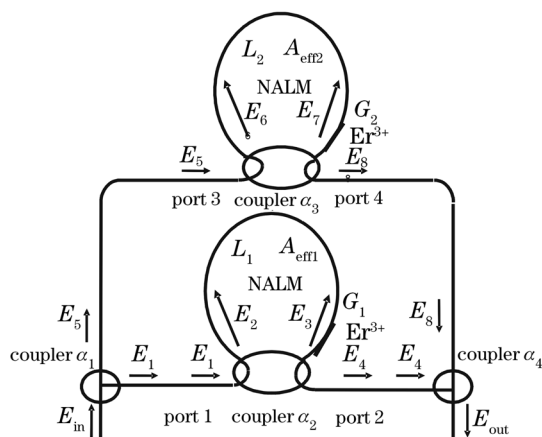


Fig. 3. Two NALMs in parallel.

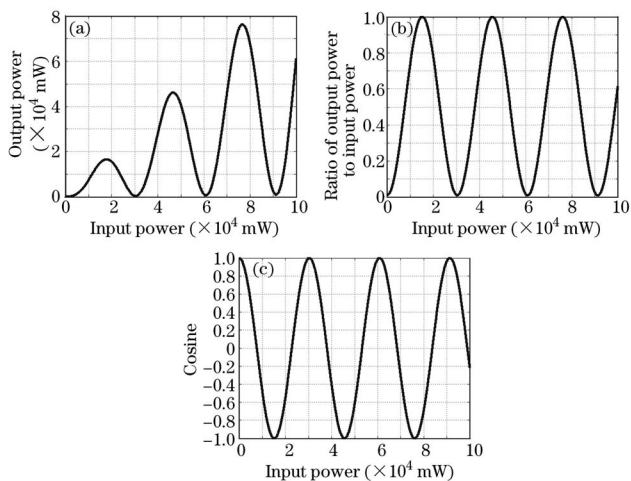


Fig. 4. (a) Output power versus input power; (b) ratio of output power to input power; (c) cosine switching. $L = 200$ m, $a = 2$ μ m, $\alpha = 0.45$.

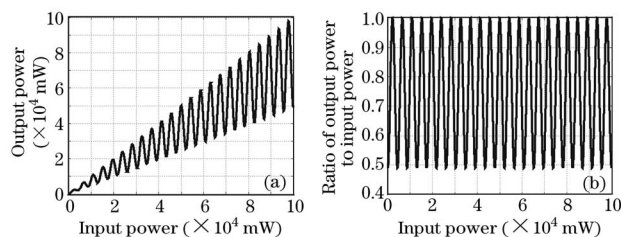


Fig. 5. (a) Output power versus input power; (b) ratio of output power to input power. $L = 200$ m, $a = 2$ μ m, $\alpha = 0.15$.

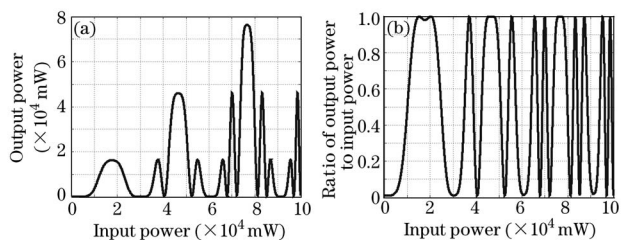


Fig. 6. $L_1 = L_2 = 200$ m, $a_1 = a_2 = 2$ μ m, $\alpha_1 = \alpha_2 = 0.45$. Loop 2.

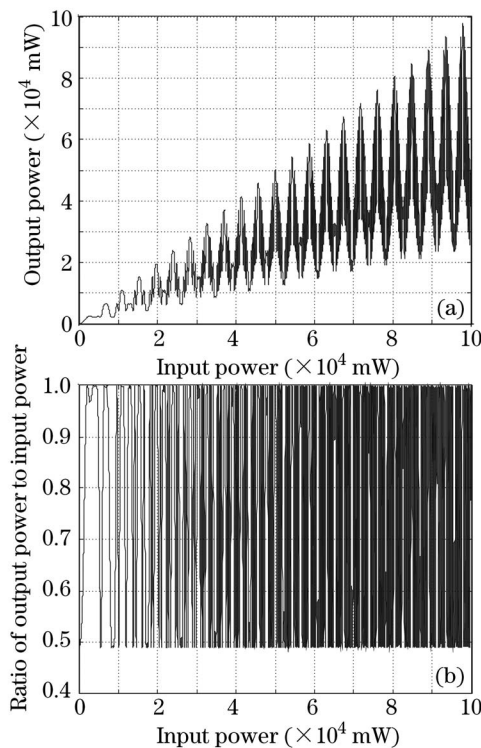


Fig. 7. $L_1 = L_2 = 200$ m, $a_1 = a_2 = 2$ μ m, $\alpha_1 = \alpha_2 = 0.15$. Loop 2.

second loop $\alpha = 0.45$, we get a different modulation pattern, as shown in Fig. 15. The high switching frequency of the first NOLM loop is modulated by the lower switching frequency of the second loop. The output power stays more or less the same. The modulation depth varies between 75% and 65%.

All in all a single NOLM loop appears to be better than two NOLM loops in parallel, if one wants to reduce the power and manipulate the modulation depth.

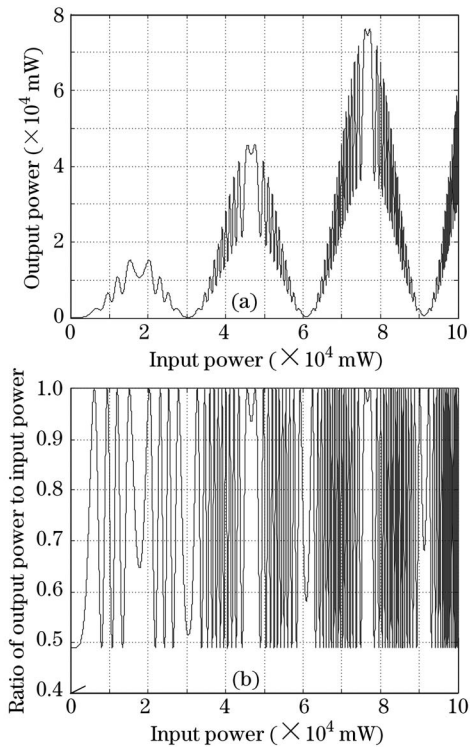


Fig. 8. $L_1 = L_2 = 200$ m, $a_1 = a_2 = 2 \mu\text{m}$, $\alpha_1 = 0.45$, $\alpha_2 = 0.15$. Loop 2.

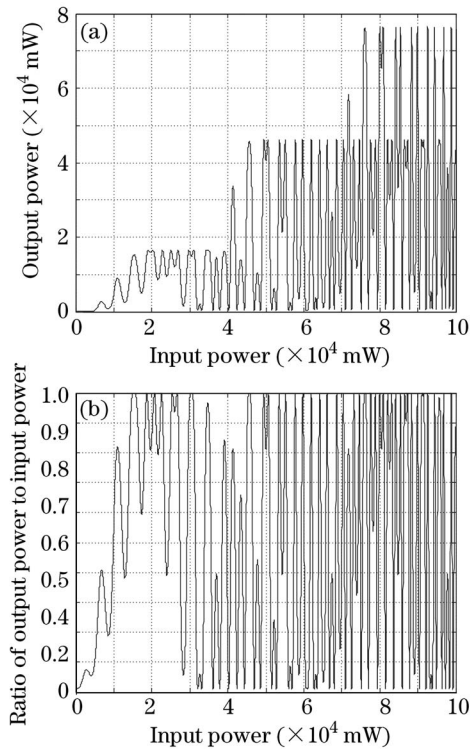


Fig. 9. $L_1 = L_2 = 200$ m, $a_1 = a_2 = 2 \mu\text{m}$, $\alpha_1 = 0.15$, $\alpha_2 = 0.45$. Loop 2.

IV Simulation results of a single NALM loop
 In a NALM loop we have gain, therefore the length of the nonlinear Kerr fiber can be much shorter and the effective fiber core area much larger. We keep the coupling

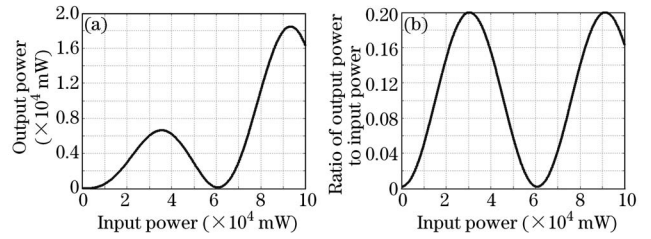


Fig. 10. $L_1 = L_2 = 200$ m, $a_1 = a_2 = 2 \mu\text{m}$, $\alpha_1 = \alpha_2 = 0.45$. Double NOLM loop parallel.

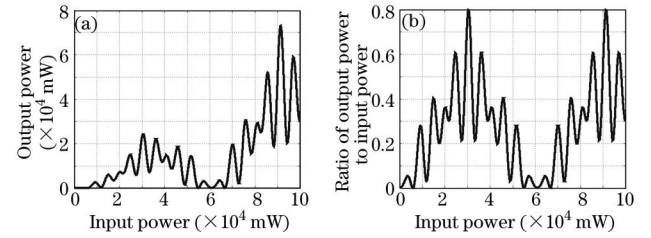


Fig. 11. $L_1 = 200$ m, $L_2 = 300$ m, $a_1 = 2 \mu\text{m}$, $a_2 = 1.4 \mu\text{m}$, $\alpha_1 = \alpha_2 = 0.45$. Double NOLM loop parallel.

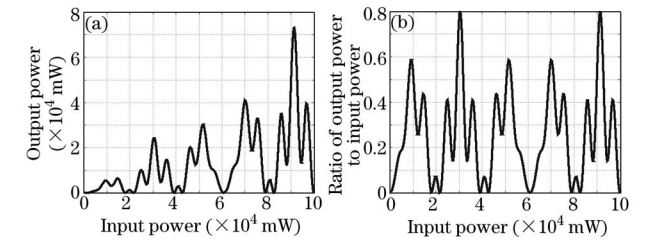


Fig. 12. $L_1 = 300$ m, $L_2 = 200$ m, $a_1 = 1.4 \mu\text{m}$, $a_2 = 2 \mu\text{m}$, $\alpha_1 = \alpha_2 = 0.45$. Double NOLM loop parallel.

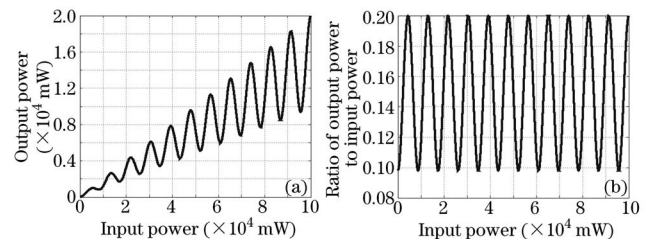


Fig. 13. $L_1 = L_2 = 200$ m, $a_1 = a_2 = 2 \mu\text{m}$, $\alpha_1 = \alpha_2 = 0.15$. Double NOLM loop parallel.

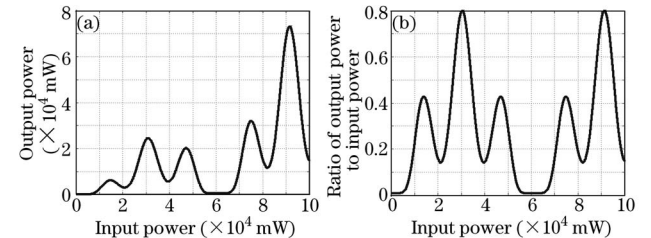


Fig. 14. $L_1 = L_2 = 200$ m, $a_1 = a_2 = 2 \mu\text{m}$, $\alpha_1 = 0.45$, $\alpha_2 = 0.15$. Double NOLM loop parallel.

constant fixed at $\alpha = 0.5$, to insure 100% modulation depth.

Figure 16(a) shows the output power versus the input power. Because of the gain, the output power is much

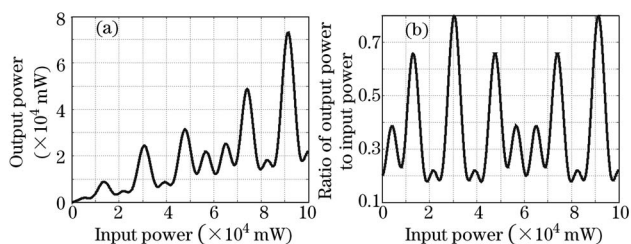


Fig. 15. $L_1 = L_2 = 200$ m, $a_1 = a_2 = 2$ μ m, $\alpha_1 = 0.15$, $\alpha_2 = 0.45$. Double NOLM loop parallel.

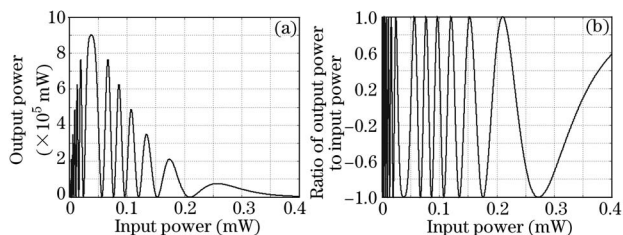


Fig. 16. (a) Output power versus input power (single loop); (b) cosine switching. $L = 35$ m, $a = 4$ μ m, $L_{Er} = 16$ m, $g_0 = 1.6 \times 0.705$.

higher than the input power. Because of gain saturation the switching stops already at low input powers. Figure 16(b) gives the cosine function which is responsible for the switching. If we increase the length of the nonlinear Kerr fiber, and/or the effective fiber core area, the switching frequency increases. If we do not increase the gain the output power stays the same. If we increase the gain, both the switching frequency and the power output increase.

V Simulation results of two NALM loops in series

Firstly we consider two equal NALM loops. In Fig. 17, compared to a single NALM loop the switching pattern is similar, but is shifted to higher input powers, in our case to between 1 and 2.5 mW, compared to 0 and 0.35 mW. At the original position between 0 and 0.35 mW some switching is observed. The output powers are the same. In Fig. 18, if in both NALM loops the length of the nonlinear Kerr fibers is increased and/or the effective areas of the fiber cores decreased, the switching frequency increases, and a further shift to higher powers is observed.

Secondly we consider two different NALM loops, as shown in Figs. 19 and 20. Compared to two equal NALM loops, the first NALM loop determines the shift to higher powers, the second loop the switching frequency. Two equal loops with the same dimensions as the first loop share the same power shift, while two equal loops with the same dimensions as the second loop share the same switching frequency.

VI Simulation results of two NALM loops in parallel

Firstly we consider two equal NALM loops. In Fig. 21, compared to a single loop, the switching frequency has increased, however, the output power is slightly lower. In Fig. 22, If the length of the nonlinear Kerr fiber is increased and/or the effective area of the fiber core decreased, the switching frequency increases, and is higher than for a single loop (see Figs. 23 and 24). To see that the switching frequency in a parallel double loop is higher, we zoom in.

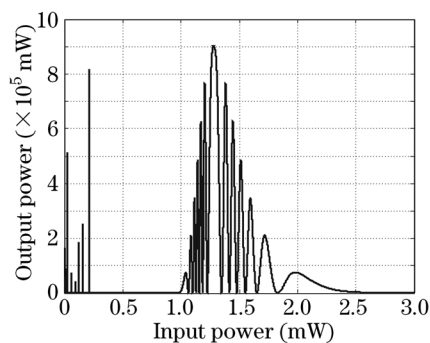


Fig. 17. Output power versus input power (loop 2). $L_1 = L_2 = 35$ m, $a_1 = a_2 = 4$ μ m.

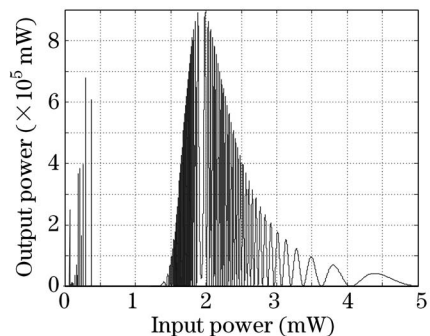


Fig. 18. $L_1 = L_2 = 100$ m, $a_1 = a_2 = 3$ μ m. Loop 2.

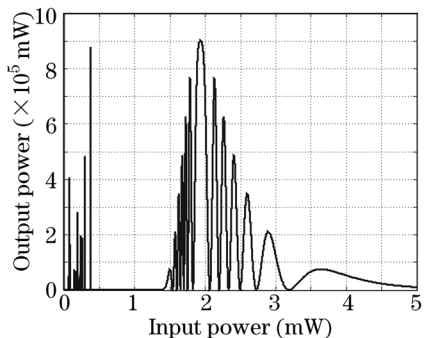


Fig. 19. $L_1 = 100$ m, $L_2 = 35$ m, $a_1 = 3$ μ m, $a_2 = 4$ μ m. Loop 2.

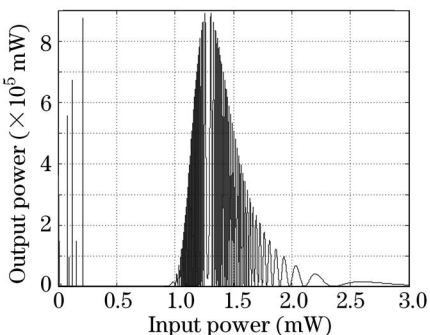


Fig. 20. $L_1 = 35$ m, $L_2 = 100$ m, $a_1 = 4$ μ m, $a_2 = 3$ μ m. Loop 2.

Secondly we consider two different NALM loops, as shown in Figs. 25 and 26. If the length of the nonlinear Kerr fiber of the first loop is increased and/or the effective area of the fiber core decreased, the switching frequency increases.

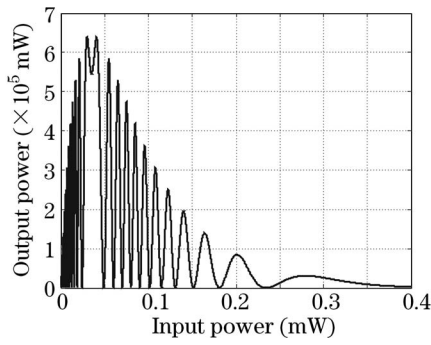


Fig. 21. $L_1 = L_2 = 35$ m, $a_1 = a_2 = 4$ μ m. Double NALM loop parallel.

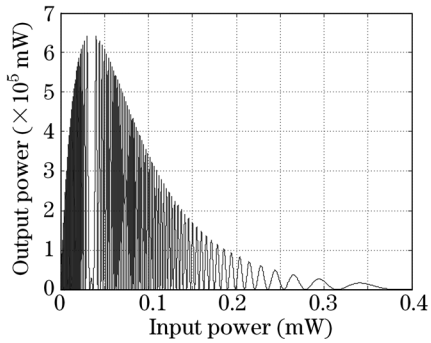


Fig. 22. $L_1 = L_2 = 100$ m, $a_1 = a_2 = 3$ μ m. Double NALM loop parallel.

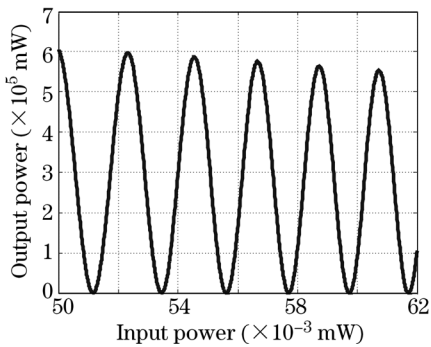


Fig. 23. $L_1 = L_2 = 35$ m, $a_1 = a_2 = 4$ μ m. Double NALM loop parallel.

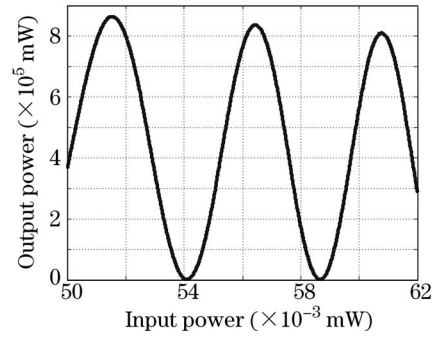


Fig. 24. $L = 35$ m, $a = 4$ μ m. Single loop.

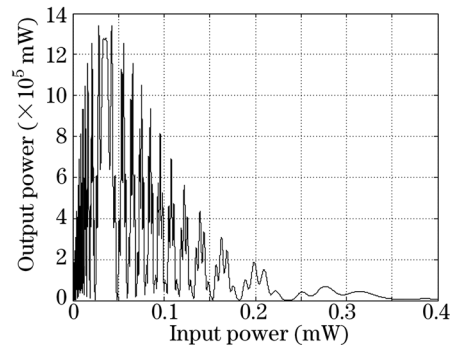


Fig. 25. $L_1 = 35$ m, $L_2 = 100$ m, $a_1 = 4$ μ m, $a_2 = 3$ μ m. Double NALM loop parallel.

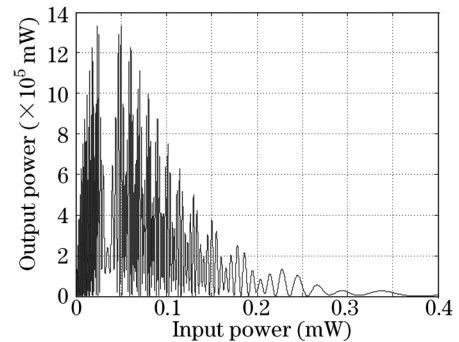


Fig. 26. $L_1 = 100$ m, $L_2 = 35$ m, $a_1 = 3$ μ m, $a_2 = 4$ μ m. Double NALM loop parallel.

In conclusion, we have developed the switching equations for a single NOLM loop, as well as for two NOLM loops in series and in parallel. We investigated the switching behavior in dependence of the lengths of the nonlinear Kerr fibers, the effective fiber core areas, and the coupling constants.

Furthermore, we derived the switching equations for a single NALM loop, as well as for two NALM loops in series and in parallel. Here we studied the switching behavior in dependence of the lengths of the nonlinear Kerr fibers, the effective fiber core areas, and the gains. We found that we can design the switching frequency we want by selecting the corresponding configurations. Especially, with two NOLM loops in series we find high switching frequencies and 100% modulation depth by

selecting for the two NOLM loops different coupling constants. A single NALM loop becomes unstable at high pump powers, by arranging multiple loops in parallel we are able to keep the power in a single loop low, while the total power output is high.

D. Schmieder's e-mail address is ds@ing.rau.ac.za, P. L. Swart's e-mail address is pls@ing.rau.ac.za.

References

1. N. J. Doran and D. Wood, *Opt. Lett.* **13**, 1 (1988).
2. M. E. Fermann, F. Haberl, M. Hofer, and H. Hochreiter, *Opt. Lett.* **15**, 13 (1990).
3. C. Rullière (eds.) *Femtosecond Laser Pulses: Principles and Experiments* (Springer-Verlag, Berlin, 1998).